




# In situ synthesis of Co-doped MoS<sub>2</sub> nanosheet for enhanced mimicking peroxidase activity

Qiqi Zhu<sup>1</sup>, Hua Zhang<sup>1</sup>, Yingchun Li<sup>2,3</sup>, Hui Tang<sup>1</sup>, Jia Zhou<sup>2</sup>, Yifan Zhang<sup>1</sup>, and Jiao Yang<sup>2,\*</sup> 

<sup>1</sup>Key Laboratory of Xinjiang Phytomedicine Resources for Ministry of Education, School of Pharmacy, Shihezi University, Shihezi 832000, China

<sup>2</sup>College of Science, Harbin Institute of Technology, Shenzhen 518055, China

<sup>3</sup>College of Optoelectronic Engineering, Shenzhen University, Shenzhen 518060, China

Received: 10 November 2021

Accepted: 5 April 2022

Published online:  
25 April 2022

© The Author(s), under exclusive licence to Springer Science+Business Media, LLC, part of Springer Nature 2022

## ABSTRACT

To enhance the catalytic activity of two-dimensional layered materials as versatile materials, the modification of transition metal dichalcogenide nanosheets such as MoS<sub>2</sub> by doping with heteroatoms has drawn great interests. However, few reports are available on the study of the enzyme-like activity of doped MoS<sub>2</sub>. In this study, a facile in situ hydrothermal method for the preparation of various ultrathin transition metals (Fe, Cu, Co, Mn, and Ni) doped MoS<sub>2</sub> nanosheets has been reported. Through the density functional theory (DFT) and steady-state kinetic analysis, the Co-doped MoS<sub>2</sub> nanosheets exhibited the highest peroxidase-like catalytic activity among them. Furthermore, a typical colorimetric assay for H<sub>2</sub>O<sub>2</sub> was presented based on the catalytic oxidation of colorless 3,3',5,5'-tetramethylbenzidine (TMB) to a blue product (oxTMB) by Co-MoS<sub>2</sub>. The proposed colorimetric method showed excellent tolerance under extreme conditions and a broad linear range from 0.0005 to 25 mM for H<sub>2</sub>O<sub>2</sub> determination. Concerning the practical application, in situ detection of H<sub>2</sub>O<sub>2</sub> generated from SiHa cells was also fulfilled, fully confirming the great practicability of the proposed method in biosensing fields.

Handling Editor: Mark Bissett.

Qiqi Zhu and Hua Zhang have contributed equally to this work.

Address correspondence to E-mail: yang21803@hotmail.com

## Introduction

With the development of nanotechnology, nanomaterial-based enzyme mimics (nanozyme) are widely used as alternatives to natural enzymes because of their attractive merits of outstanding tolerance in harsh environments, easy large-scale production, and low cost. The reported enzyme-like activities include the peroxidase-like activity [23], superoxide dismutase-like activity [7], catalase-like activity [17], and so on. The unique characteristics of nanomaterials and the synergistic effect of enzyme-like activities, making nanozymes potential applications in wide fields including biosensing [34], food industry, pharmaceutical processes, and environmental treatment [36]. Since the first research that  $\text{Fe}_3\text{O}_4$  nanoparticles possess an intrinsic peroxidase activity [8], an emerging class of nanomaterials such as transition metal oxides/chalcogenides [5, 28, 35], noble metal [3, 22, 32], carbon-based materials [37], metal–organic framework (MOF) [20], and others [16, 25] have been explored as nanozymes.

Recently, two-dimensional (2D) layered materials are attracting in sensing fields due to their unique physicochemical properties originating from their chemical structure [12]. Among them, molybdenum disulfide ( $\text{MoS}_2$ ), one of typical 2D materials, has drawn remarkable attentions due to its tunable energy bandgap, intrinsic catalytic activity, durable stability, and natural richness [1]. Each plane is composed by S-Mo-S sandwich-layered structure with weak van der Waals force between layers, which endows  $\text{MoS}_2$  with graphene-like characteristics, such as unique electronic, high surface area, optical, and chemical properties [19, 33]. Lots of studies reported that the coordinatively unsaturated S/Mo atoms located at the edges of  $\text{MoS}_2$  nanosheets are active for many catalytic reactions, while the S atoms in-plane domains are usually inserted [10]. However, with the inherent tendency of anisotropic bonding and surface energy minimization, the edges are regular scarce domains of layered materials [29]. Numerous efforts have been made to improve the intrinsic activity of  $\text{MoS}_2$ , including elemental doping, conversion from 2H to 1T, compounding with other materials, etc. [4, 27, 31]. In nanozyme field, the most used improvement of  $\text{MoS}_2$  is hybridization with other nanomaterials. Cai's group has designed  $\text{Pt}_{74}\text{Ag}_{26}$  bimetallic nanoparticle-decorated  $\text{MoS}_2$

nanosheets for colorimetric determination of  $\text{H}_2\text{O}_2$  and glucose [2]. Ma's group has prepared  $\text{MoS}_2$ -Au composite with peroxidase-like activity for highly sensitive colorimetric detection of  $\text{Hg}^{2+}$  [21]. Although these composites demonstrated significant enhancement on enzyme-like catalytic activity compared to pure  $\text{MoS}_2$ , their preparation processes are complicated. Single metal atom doping is considered to be a facile and effective technique to enhance the catalytic activity of  $\text{MoS}_2$  by allowing the insertion of the original S atom near the doped metal atoms. In natural enzymes, transition metal ions are wrapped around protein substrates as part of metal macrocyclic complexes and exhibit ultra-high catalytic activity and selectivity in biological systems. During enzyme catalysis, the peptide and residue functional groups surrounding the enzyme control the electron density of the active site to an appropriate value matching the energy level of the substrate (reacting species), enabling the transfer of electrons from substrate to product [26]. Li's group reported that Al-doped  $\text{MoS}_2$  provided an enhanced catalytic activity for CO oxidation, in which the Al atom doping obviously reduced the band structure and enhanced the conductivity [18]. Shi et al. tuned the energy level of  $\text{MoS}_2$  via doping with Zn atom, which could accelerate the hydrogen evolution reaction and decrease onset potential [26]. Raza et al. reported that Co-doped  $\text{MoS}_2$  exhibited improved efficiency for methylene blue degradation [24]. Lei et al. designed an ultrasensitive dopamine sensor based on Mn-doped  $\text{MoS}_2$  [13]. As far as we know, there was no study explored to investigate the enzyme-like activity of transition metal-doped  $\text{MoS}_2$ .

Hydrogen peroxide ( $\text{H}_2\text{O}_2$ ) is not only a by-product of several highly selective enzymes, but also can be considered as a biomarker for cancer, Alzheimer's and Parkinson's due to its damage to tissues and cells [6, 11, 15]. Its rapid and precise detection is therefore a fundamental issue. To date, colorimetric technique for  $\text{H}_2\text{O}_2$  detection has particularly attracted wide attentions for point-of-care applications attributed to their great advantages involving simplicity, sensitivity, and low cost [30]. Therefore, in this work, we studied the colorimetric sensing of  $\text{H}_2\text{O}_2$  using Co-doped  $\text{MoS}_2$ . Initially, one-step in situ hydrothermal method was utilized for preparation of a serial transition metal-doped  $\text{MoS}_2$ . Interestingly and expectantly, the results showed that the Co-doped  $\text{MoS}_2$  exhibited superior enzyme-like catalytic activity

toward  $\text{H}_2\text{O}_2$ . The main reason for the highest peroxidase-like activity of Co-doped  $\text{MoS}_2$  among various transition metal-doped  $\text{MoS}_2$  including Mn, Ni, Cu, and Fe was revealed by density functional theory (DFT) as well as steady-state kinetic analysis. In addition, determination method of  $\text{H}_2\text{O}_2$  catalyzed by Co-doped  $\text{MoS}_2$  as mimetic peroxidase was then established based on colorimetry. In situ measurement of  $\text{H}_2\text{O}_2$  generated from SiHa cells was also fulfilled, expanding the application of Co-doped  $\text{MoS}_2$  nanosheets in biosensing fields.

## Experimental section

### Reagents and apparatus

L-Cysteine,  $\text{Co}(\text{NO}_3)_2 \cdot 6\text{H}_2\text{O}$ ,  $\text{FeSO}_4 \cdot 7\text{H}_2\text{O}$ ,  $\text{CuSO}_4 \cdot 5\text{H}_2\text{O}$ ,  $\text{NiCl}_2 \cdot 6\text{H}_2\text{O}$ ,  $\text{Mn}(\text{NO}_3)_2 \cdot 4\text{H}_2\text{O}$ , sodium acetate (NaAc), acetic acid (HAc, 99.5%), and dihydroethidium (HE) were purchased from Adamas Reagent Co. Ltd. (Shanghai, China). *p*-benzoquinone (BQ), isopropanol alcohol (IPA), and terephthalic acid (TA) were supplied by Titan Scientific Co., Ltd. (Shanghai, China; [www.tansoole.com](http://www.tansoole.com)) Sodium molybdenum oxide ( $\text{Na}_2\text{MoO}_4$ ) was obtained from Alfa Aesar (Shanghai, China). 30% hydrogen peroxide ( $\text{H}_2\text{O}_2$ ) was supplied by Sigma-Aldrich (USA). 3,3',5,5'-Tetramethylbenzidine (TMB, 99%), phosphate-buffered saline (PBS, 0.01 M, pH 7.0), fetal bovine serum (FBS), and phorbol 12-myristate 13-acetate (PMA) were bought from Sangon Biotechnology Co., Ltd. (Shanghai, China). The  $\text{H}_2\text{O}_2$  assay kit was obtained from Jiancheng Bioengineering Institute (Nanjing, China). Other reagents such as glucose, urea, and uric acid were of at least analytical grade and used as-received. The pH value of HAc-NaAc buffer solution (0.1 M) was adjusted by HAc or NaOH (5 M). TMB solution (10 mM) was freshly prepared by dissolving TMB in anhydrous ethanol. Ultrapure water (18.2 M $\Omega$  cm) used in the whole experiments was obtained by Millipore ultrapure system.

Surface morphologies of the prepared  $\text{MoS}_2$  were identified by transmission electron microscopy (TEM, FEI spirit T12, USA) by drying 10  $\mu\text{L}$  sample solution on Cu-grids with carbon film. Field emission scanning electron microscopy (FE-SEM) images were obtained on ITO-glass using Hitachi S-4800 (Japan). X-ray diffraction (XRD) was operated on an UltimaIV X-ray Cu K $\alpha$  radiation diffractometer for element

analysis by drying sample solution on ITO-glass. X-ray photoelectron spectroscopy (XPS) measurement, which was used for elemental analysis, was performed on Thermo ESCALAB 250XI. All colorimetric measurements were performed on UV-2600 ultraviolet–visible (UV–Vis) spectrometer (Shimadzu, Kyoto, Japan). Steady-state kinetic assays and fluorescence spectra were recorded by Synergy<sup>TM</sup> HTX Multi-Mode microplate reader (Biotek Instruments, USA).

### Materials synthesis

$\text{MoS}_2$ -based materials were synthesized according to a modified one-pot hydrothermal route reported by Guo et al. [9]. For preparation of pure  $\text{MoS}_2$ , an aqueous solution of 2.0 mM  $\text{Na}_2\text{MoO}_4$  and 4.0 mM L-cysteine was stirred at room temperature for 15 min and then transferred into a 100 mL Teflon-lined stainless-steel autoclave. The autoclave was heated at 200 °C for 12 h and cooled down to room temperature naturally. Subsequently, the as-obtained product was collected by centrifugation with a speed of 12,000 rpm for 20 min. The precipitate was washed with DI water for three times and re-dispersed in 50 mL DI water. Besides, Co-, Fe-, Cu-, Ni-, and Mn-doped  $\text{MoS}_2$  nanomaterials were synthesized using the same method as above in the presence of 0.15 mM of the corresponding metal ion ( $\text{Co}(\text{NO}_3)_2$ ,  $\text{FeSO}_4$ ,  $\text{CuSO}_4$ ,  $\text{NiCl}_2$ , and  $\text{Mn}(\text{NO}_3)_2$ ) in a mixed solution of  $\text{Na}_2\text{MoO}_4$  and L-cysteine, respectively.

### The peroxidase-like activity of Co-doped $\text{MoS}_2$

The spectroscopic determination of  $\text{H}_2\text{O}_2$  by Co-doped  $\text{MoS}_2$  was investigated as follows: 1.375 mL NaAc (0.1 M, pH 4.0) buffer was mixed with 50  $\mu\text{L}$  Co- $\text{MoS}_2$  (0.325 mg/mL) and 10  $\mu\text{L}$   $\text{H}_2\text{O}_2$  (1 mM), and then, 75  $\mu\text{L}$  TMB (0.5 mM) was added immediately and mixed with vortex mixer. After reaction for 10 min, the UV–Vis absorption spectra were recorded at 652 nm. The concentration of Co-doped  $\text{MoS}_2$  was optimized by similar procedure except that the dosage of Co-doped  $\text{MoS}_2$  (0–100  $\mu\text{L}$ ) was changed. The influence of pH and temperature on catalytic activity of Co-doped  $\text{MoS}_2$  was also inquired by the above-mentioned method, expect that the pH value (3.0–10.0) and temperatures (4–50 °C) of the reaction solution were varied, respectively. For each

determination, three independent measurements were conducted.

### Steady-state kinetic assays

Steady-state kinetic measurements of the catalytic reactions were conducted at room temperature in 96-well plates with 200  $\mu\text{L}$  reaction solution (0.1 M NaAc, pH 4.0) with 7.1  $\mu\text{L}$  Co-doped  $\text{MoS}_2$  (0.325 mg/mL) in the presence of 10  $\mu\text{L}$  TMB (10 mM) and different concentrations of  $\text{H}_2\text{O}_2$  (5, 10, 20, 30, 40, 50, 75, 125, 250, 375 mM), while for TMB as the substrate, the kinetic assay was performed by a similar method with diverse TMB concentrations (0.1–1 mM) in the presence of 10 mM  $\text{H}_2\text{O}_2$ . All reactions were performed by measuring the absorbance at 652 nm ( $A_{652\text{nm}}$ ) at various reaction times. The obtained  $A_{652\text{nm}}$  were back-converted to oxTMB concentration by Beer–Lambert law,  $A = \epsilon bC$ , where the molar absorption coefficient  $\epsilon$  was 39,000  $\text{M}^{-1} \text{cm}^{-1}$ , and path length of vitric cuvette  $b$  was 0.625 cm. Kinetic parameters were calculated according to the Michaelis–Menten equation:  $1/v = K_m/V_m[S] + 1/V_m$ , in which  $v$  is the initial velocity, which can be calculated by the initial slope of  $A_{652\text{nm}}$  changes with time,  $V_{\text{max}}$  is the maximum velocity,  $[S]$  is the concentration of substrate ( $\text{H}_2\text{O}_2$  or TMB), and  $K_m$  is the Michaelis–Menten constant.

### Performance of Co-doped $\text{MoS}_2$ on $\text{H}_2\text{O}_2$ determination

For quantitative analysis of  $\text{H}_2\text{O}_2$ , the colorimetric assay was performed at 25  $^\circ\text{C}$  in a 1.5 mL reaction buffer solution (0.1 M acetate buffer, pH 4.0) containing 50  $\mu\text{L}$  Co-doped  $\text{MoS}_2$  (0.325 mg/mL) as catalyst in the presence of different concentrations of  $\text{H}_2\text{O}_2$ , and then, 75  $\mu\text{L}$  TMB (0.5 mM) was added and mixed immediately. After 10 min incubation, the spectrophotometric measurement was recorded at 652 nm. Three independent measurements were performed for each  $\text{H}_2\text{O}_2$  concentration.

### Real sample detection

SiHa cells were purchased from the Chinese Academy of Sciences Cell Bank. They were cultured in Dulbecco's modified eagle medium (supplemented with 10% FBS, and 1% penicillin/streptomycin) and maintained in an atmosphere of 5%  $\text{CO}_2$  at 37  $^\circ\text{C}$ . In

order to assess the release of  $\text{H}_2\text{O}_2$  from SiHa cells, the cells ( $4 \times 10^4$  cells/plate) were dropped into 96-well microplate for 12 h and then washed three times with PBS solution. After that, 20  $\mu\text{L}$  of PMA solution (75 ng/mL) and 80  $\mu\text{L}$  of PBS were added successively and incubated for 30 min. Furthermore, Co-doped  $\text{MoS}_2$  (0.325 mg/mL, 10  $\mu\text{L}$ ), TMB (50  $\mu\text{L}$ , 0.5 mM), and acetate buffer (100  $\mu\text{L}$ , pH 4.0) were added subsequently for incubation 10 min. Finally, the absorbances at 652 nm were recorded by a microplate reader.

## Results and discussion

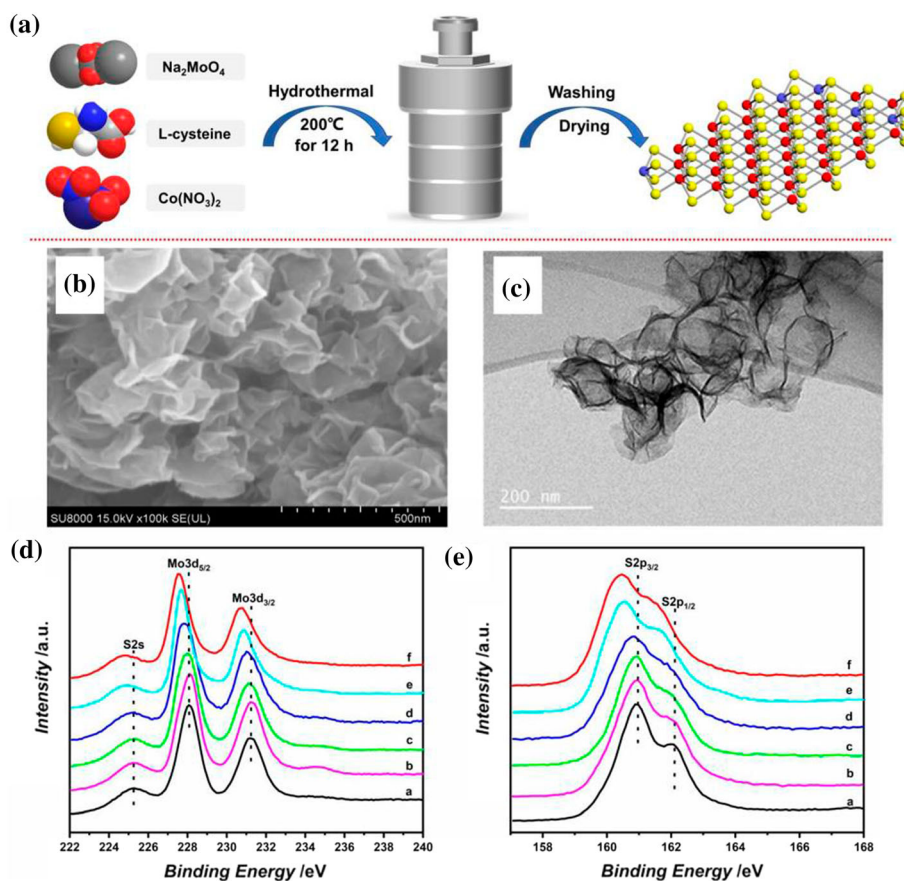
### Synthesis and characterization of Co-doped $\text{MoS}_2$

The Co-doped  $\text{MoS}_2$  materials were prepared by a one-pot hydrothermal method using  $\text{Na}_2\text{MoO}_4$  and  $\text{Co}(\text{NO}_3)_2$  as precursors and L-cysteine as a reductant (Fig. 1a). The scanning electron microscopy (SEM) images (Fig. 1b) display Co-doped  $\text{MoS}_2$  consisting of a fairly homogeneous two-dimensional nanosheets structure with high surface area and volume-to-surface ratio. Similar structures also appear in  $\text{MoS}_2$  and other transition metals (Ni, Fe, Cu, Mn)-doped  $\text{MoS}_2$  (Fig. S1A–E). An ultrathin lamellar structure with ample graphene-like wrinkles and folds is observed in transmission electron microscopy (TEM) image (Fig. 1c), further implying the typical two-dimensional nanosheets structure of Co-doped  $\text{MoS}_2$ .

The typical X-ray diffraction (XRD) patterns of  $\text{MoS}_2$  and Co-doped  $\text{MoS}_2$  are shown in Fig. S2. A diffraction peak at 14.4 $^\circ$  can be well indexed to (002) of  $\text{MoS}_2$  (JCPDS card no. 37–1492) and Co-doped  $\text{MoS}_2$  [14, 19]. There is no other crystal phase observed after Co doping except the intensity of (002) increased, indicating the Co doping can enhance the crystal phase of  $\text{MoS}_2$ . The composition of obtained Co-doped  $\text{MoS}_2$  was further verified by X-ray photoelectron spectroscopy (XPS). As shown in Fig. S3, combined with the overall XPS spectrum and the high-resolution XPS spectra of each doping element, the successful doping of Co and other transition metals into  $\text{MoS}_2$  was demonstrated. The content of Co incorporation in Co-doped  $\text{MoS}_2$  is calculated as 1.3 atom %. It is noteworthy that the characteristic signal of O 1s is detected probably from the adsorbed  $\text{O}_2$  on the surface of  $\text{MoS}_2$ . Besides, from the high-



**Figure 1** **a** Schematic description of the Co-doped MoS<sub>2</sub> synthesis process. **b** SEM and **c** TEM images of Co-doped MoS<sub>2</sub>. The high-resolution XPS spectra of **d** Mo3d and **e** S2p. **a–f** stands for pure MoS<sub>2</sub>, Mn-doped MoS<sub>2</sub>, Fe-doped MoS<sub>2</sub>, Ni-doped MoS<sub>2</sub>, Cu-doped MoS<sub>2</sub>, and Co-doped MoS<sub>2</sub>, respectively



resolution spectra of Mo 3d (Fig. 1d) and S 2p (Fig. 1e), the binding energy of Co-doped MoS<sub>2</sub> shows a huge shift compared with that of MoS<sub>2</sub>. In Fig. 1d, Co-doped MoS<sub>2</sub> displays two main peaks at 227.7 and 230.8 eV, originating from the doublet of Mo 3d<sub>5/2</sub> and Mo 3d<sub>3/2</sub> (curve f). It is clear that these two peaks are negatively shifted by 0.4 eV when compared to pure MoS<sub>2</sub>. In Fig. 1e, the binding energies of S 2p<sub>3/2</sub> and S 2p<sub>1/2</sub> are negatively shifted by 0.5 eV after Co incorporation. The similar phenomenon is also discovered in Ni-doped MoS<sub>2</sub> (curve d) and Cu-doped MoS<sub>2</sub> (curve e), indicating the increased electronic density in MoS<sub>2</sub> after these elements' doping [26].

### Mimic enzymatic activity investigation

To study the enzyme-like activity of Co-doped MoS<sub>2</sub> nanosheets, catalytic reaction was performed in the presence of H<sub>2</sub>O<sub>2</sub> with TMB as substrate. As displayed in Fig. 2a, with the coexistence of TMB, H<sub>2</sub>O<sub>2</sub>, and Co-MoS<sub>2</sub> (curve a), a remarkable color change occurs and a strong absorbance appears at

652 nm, whereas the control experiments show negligible absorbance in the absence of Co-doped MoS<sub>2</sub> or H<sub>2</sub>O<sub>2</sub> (curve b, c, d). This result indicates the peroxidase-like activity of Co-doped MoS<sub>2</sub> nanosheets, which can catalyze the oxidation of colorless TMB to blue oxTMB with the help of H<sub>2</sub>O<sub>2</sub>. Furthermore, the peroxidase-like activities of MoS<sub>2</sub> doped with various transition metal atoms were studied (Fig. 2b). Compared with pure MoS<sub>2</sub>, the catalytic activities of Fe-doped MoS<sub>2</sub>, Cu-doped MoS<sub>2</sub>, and Co-doped MoS<sub>2</sub> toward H<sub>2</sub>O<sub>2</sub> are enhanced significantly, and Co-doped MoS<sub>2</sub> material possesses the highest activity. In contrast, Ni-doped MoS<sub>2</sub> and Mn-doped MoS<sub>2</sub> show suppressive absorbance at 652 nm. To reveal the enhancement in the peroxidase-like activity of Co-doped MoS<sub>2</sub>, the density of states (DOS) was calculated by DFT and a (3 × 3 × 1) Monkhorst–Pack mesh was used for the Brillouin-zone integrations to be sampled (Fig. S4). As shown in Fig. 3, the DOS of transition metal-doped MoS<sub>2</sub> around the Fermi level increases in varying degrees compared to MoS<sub>2</sub>, suggesting the doping of transition metal increases the metallicity of

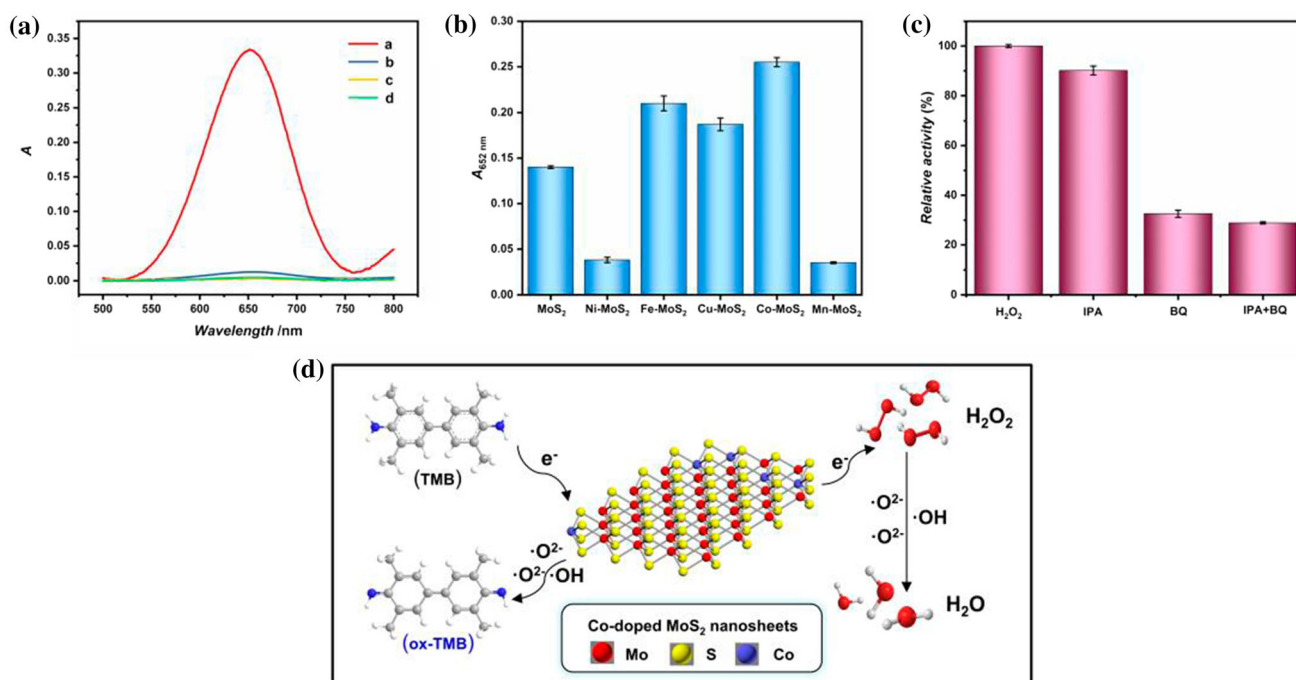


**Figure 2** **a** UV–Vis spectra of HAC–NaAc buffer solution (0.1 M, pH 4.0) containing **a** 1 mM H<sub>2</sub>O<sub>2</sub> + 0.5 mM TMB + Co-doped MoS<sub>2</sub>, **b** 1 mM H<sub>2</sub>O<sub>2</sub> + 0.5 mM TMB, **c** 0.5 mM TMB + Co-doped MoS<sub>2</sub>, **d** 0.5 mM TMB, respectively. **b** The effect of doping element on peroxidase-like activity. **c** In the coexistence system of

1 mM H<sub>2</sub>O<sub>2</sub>, 0.5 mM TMB, 0.325 mg/mL Co-doped MoS<sub>2</sub>, and 0.1 M HAC–NaAc buffer (pH 4.0), the relative activity changed after adding 10 mM IPA or BQ. **d** Schematic description of Co-MoS<sub>2</sub> nanosheets exerting peroxidase-like activity

MoS<sub>2</sub>, which in turn leads to easier electron escape. The distribution of projected density of states (PDOS) further proves that the doped metal can act as active sites for the interaction with the substrate. The d-band center is generally used to indicate the ability of a substance to adsorb and desorb reactants. The farther the d-band center is from the Fermi level, the more favorable the desorption of reactants, while the opposite is true for the adsorption of reactants. Herein, the d-band centers of Ni-doped MoS<sub>2</sub> and Co-doped MoS<sub>2</sub> are  $-0.697$  eV and  $-0.728$  eV, respectively. Combined with their higher density of states at the Fermi energy level, it is assumed that they should have higher catalytic activity. These results of DFT are consistent with that of XPS analysis.

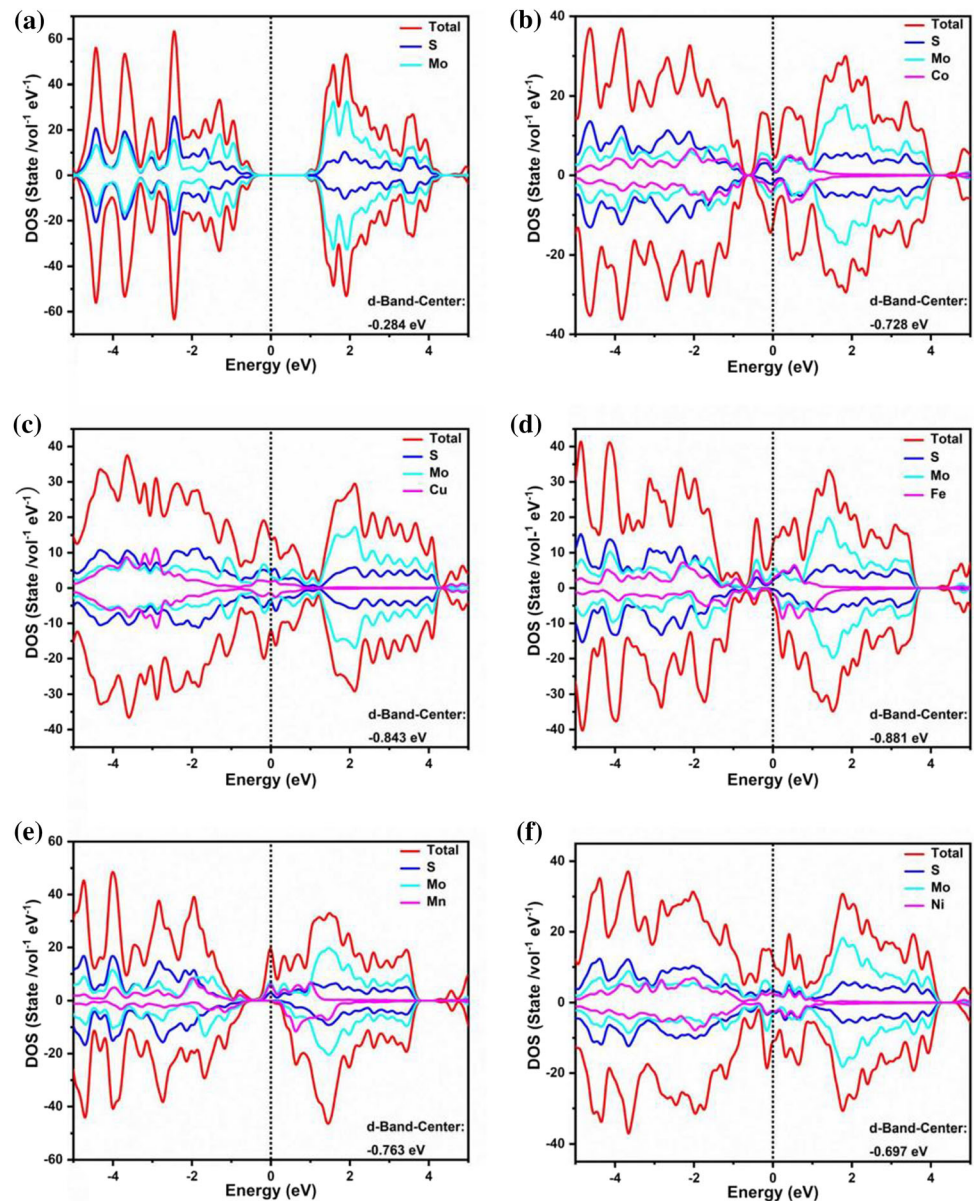
In general, reactive oxygen species like hydroxyl radical (•OH) and superoxide radical (•O<sub>2</sub><sup>-</sup>) could be easily generated from H<sub>2</sub>O<sub>2</sub> in nanozyme catalytic reaction. Therefore, to understand the possible catalytic mechanism of peroxidase-like activity, different scavengers (IPA as •OH scavenger and BQ as •O<sub>2</sub><sup>-</sup> scavenger) were added to the reaction system. As shown in Fig. 2c, it is obvious that the significant

decrease in the relative activity of Co-doped MoS<sub>2</sub> nanosheets comes alongside the addition of BQ, while for IPA, the change is weak. This result suggests that •O<sub>2</sub><sup>-</sup> plays a major role in the catalytic system. Additionally, TA and HE were employed as fluorogenic indicators for •OH and •O<sub>2</sub><sup>-</sup> to identify the type of radicals produced in the catalytic reaction. When Co-doped MoS<sub>2</sub> nanosheets and H<sub>2</sub>O<sub>2</sub> co-existed, a strong fluorescent signal was observed at 610 nm with the addition of HE (Fig. S5A), while little change in fluorescent signal was found at 380 nm after adding TA (Fig. S5B). This result further reveals that the catalytic behavior of Co-doped MoS<sub>2</sub> is due to the production of •O<sub>2</sub><sup>-</sup> and •OH, and the former exerts a greater influence on the activity of peroxidase-like enzymes. The catalytic process of Co-doped MoS<sub>2</sub> nanosheets is demonstrated in Fig. 2d.

### Optimization of assay condition

In order to demonstrate the best performance of this colorimetric assay, the preparation and reaction conditions were optimized. Firstly, the effect of doping amount on the catalytic activity of Co-doped

**Figure 3** The DOS and d-band center of **a** MoS<sub>2</sub> (001), **b** Co-doped MoS<sub>2</sub> (001), **c** Cu-doped MoS<sub>2</sub> (001), **d** Fe-doped MoS<sub>2</sub> (001), **e** Mn-doped MoS<sub>2</sub> (001), and **f** Ni-doped MoS<sub>2</sub> (001) by DFT

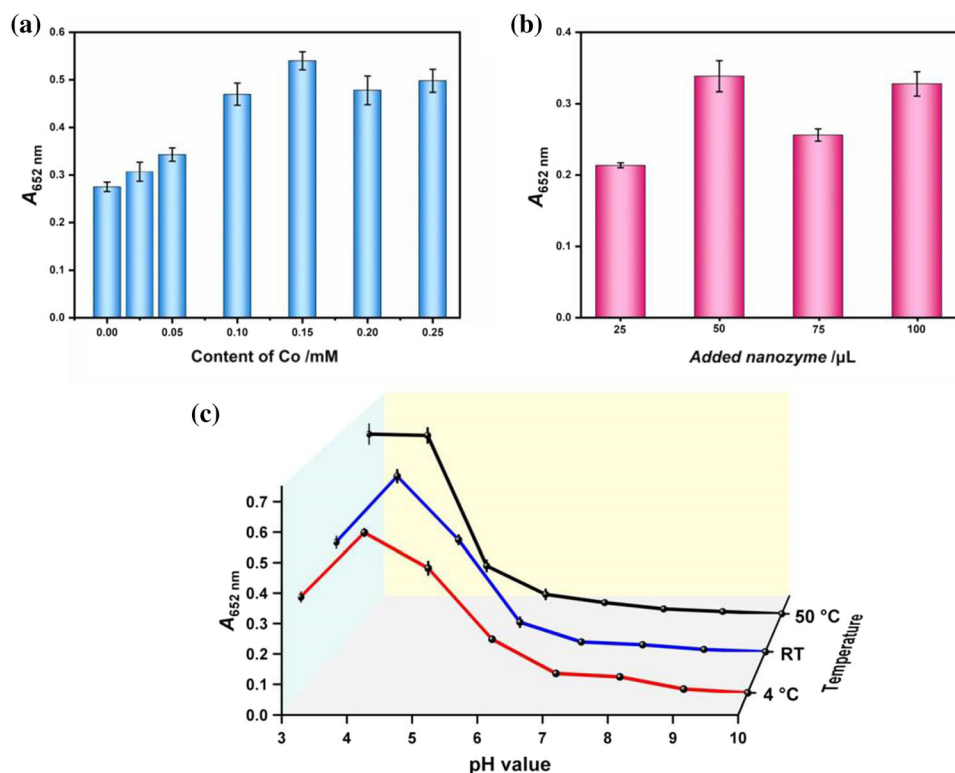


MoS<sub>2</sub> was investigated (Fig. 4a). The concentrations of Co<sup>2+</sup> in precursor are varying from 0 to 0.25 mM. From Fig. 4a, the value of  $A_{652\text{nm}}$  increases obviously from 0 to 0.15 mM and then slightly decreases with the Co amount continuously increasing, which may be attributed to the fact that excessive doping amount cannot be fully incorporated into MoS<sub>2</sub>. Therefore, Co doping amount was set as 0.15 mM. As is known to all, dosage of the catalyst is crucial for catalytic reaction, and the influence of different concentrations of Co-doped MoS<sub>2</sub> was studied (Fig. 4b). The absorbance intensity of reaction solution increases gradually with the increase in Co-doped MoS<sub>2</sub> concentration. Nevertheless, when the amount of Co-

doped MoS<sub>2</sub> exceeds 50  $\mu\text{L}$ , the large concentration of Co-doped MoS<sub>2</sub> tends to gather and form black flocculent precipitates under acidic conditions, resulting in an unstable absorbance of the system during the detection process, which in practice shows that the absorbance is suddenly low and high. So, 50  $\mu\text{L}$  was chosen as the optimal concentration of Co-doped MoS<sub>2</sub> nanosheets. As we know, natural enzyme (such as HRP) usually suffers from instability and inactivation under extreme conditions. In contrast, the superiority of nanozyme over natural enzyme is the tolerance and robustness under extreme determination conditions. The catalytic activity of Co-doped MoS<sub>2</sub> nanosheets was



**Figure 4** The effect of **a** content of Co, **b** dosage of Co-doped MoS<sub>2</sub>, and **c** pH and temperature on peroxidase-like activity



investigated with diverse pH values (3.0–10.0) at various temperatures (4, 25, and 50 °C). As can be seen in Fig. 4c, the peroxidase-like activity of Co-doped MoS<sub>2</sub> is much higher in acidic media (pH 3.0–5.0) than in neutral and basic conditions at all temperatures. The optimal activity is observed at pH 4.0, which is similar to that of HRP. In the case of temperature, the effect is much smaller than that of pH value, in which superior catalytic activity over a wide range of temperature even under high (50 °C) or low (4 °C) temperature conditions was shown. Thus, pH value of 4.0 and temperature of 25 °C are adopted as standard conditions for the following colorimetric analysis. Considering the above results, endurance and robustness of Co-doped MoS<sub>2</sub> as peroxidase mimetics under extreme environments are excellent.

### Steady-state kinetic assays of Co-doped MoS<sub>2</sub> nanosheets

To better understand the peroxidase-like catalytic activity of Co-doped MoS<sub>2</sub> nanosheets, it is necessary to perform apparent steady-state kinetic analysis to acquire the kinetic parameters such as Michaelis–Menten constant ( $K_m$ ) and maximum initial velocity

of the reaction ( $V_{\max}$ ). As shown in Fig. S6, typical Michaelis–Menten curves are obtained by varying concentrations of TMB or H<sub>2</sub>O<sub>2</sub> under similar conditions. A well-defined linear fit is found from the corresponding Lineweaver–Burk plots (Fig. S6B, D), and  $K_m$  and  $V_{\max}$  are calculated according to the Michaelis–Menten equation. The corresponding parameters were summarized and compared with natural horseradish peroxidase (HRP) (Table 1). It is well known that  $K_m$  represents the enzyme affinity of nanozyme to substrate. Low  $K_m$  value indicates high affinity to substrate. Co-doped MoS<sub>2</sub> demonstrates a higher affinity for TMB as well as a larger  $V_{\max}$  value for H<sub>2</sub>O<sub>2</sub> as substrate than HRP. In addition, the  $K_m$  for H<sub>2</sub>O<sub>2</sub> is much higher than that for TMB, suggesting that in high concentrations of H<sub>2</sub>O<sub>2</sub>, the Co-doped MoS<sub>2</sub> nanosheets can react with relatively low

**Table 1** Comparison of  $K_m$  and  $V_{\max}$  between Co-doped MoS<sub>2</sub> and HRP

Catalyst	$K_m$ (mM)		$V_{\max}$ ( $10^{-8}$ M/s)		Reference
	H <sub>2</sub> O <sub>2</sub>	TMB	H <sub>2</sub> O <sub>2</sub>	TMB	
Co-doped MoS <sub>2</sub>	17.9	0.16	22.3	0.85	This work
HRP	3.7	0.434	8.71	10	[8]



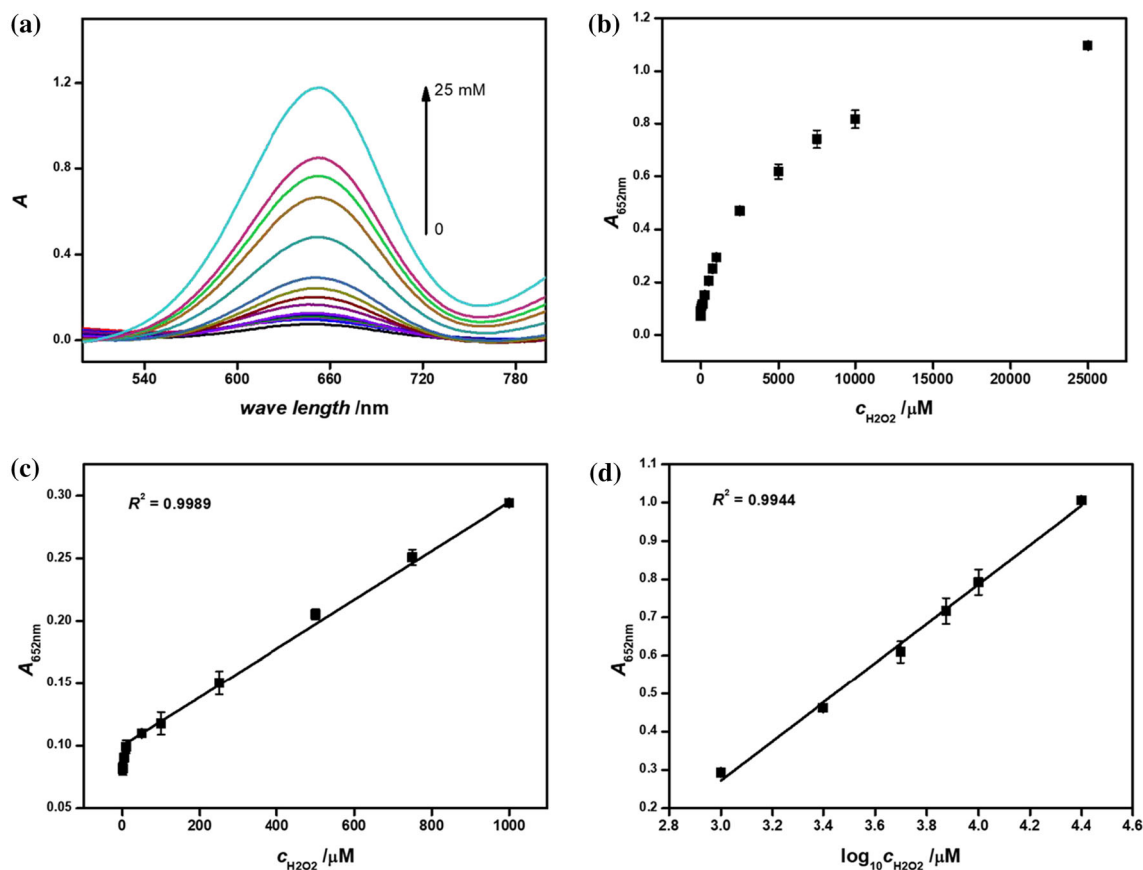


**Figure 5** a UV–Vis spectra of Co-doped MoS<sub>2</sub> measuring various concentrations of H<sub>2</sub>O<sub>2</sub> with pH of 4.0, TMB concentration of 0.5 mM, and reaction time of 10 min. b The dependency of the

absorbance at 652 nm on the H<sub>2</sub>O<sub>2</sub> concentration from 0.5 μM to 25 mM. c and d represent the calibration curves in the range of 0.5 μM to 1 mM and 1 mM to 25 mM, respectively

amount of substrate to achieve maximum catalytic activity.

Besides, the  $K_m$  and  $V_{max}$  values for each MoS<sub>2</sub> material are summarized in Table S1. From Table S1, Co-doped MoS<sub>2</sub> nanosheets have the lowest  $K_m$  and largest  $V_{max}$ , suggesting Co-doped MoS<sub>2</sub> owns the best affinity for H<sub>2</sub>O<sub>2</sub> and rapidity of the catalytic reaction. However, the  $V_{max}$  of Ni-doped MoS<sub>2</sub> is only 0.01 μM s<sup>-1</sup>, which is 7 times lower than even MoS<sub>2</sub>. Given that the Co-doped MoS<sub>2</sub> has a better performance in terms of both electron density, active site, adsorption and desorption capacity, affinity, and reaction rate, it has the highest peroxidase-like activity.

### Colorimetric detection H<sub>2</sub>O<sub>2</sub> using Co-MoS<sub>2</sub> nanosheets

Based on intrinsic peroxidase-like activity of Co-doped MoS<sub>2</sub> nanosheets, determination of H<sub>2</sub>O<sub>2</sub> was

conducted using the chromogenic reaction catalyzed by Co-doped MoS<sub>2</sub> in the presence of TMB. Figure 5a, b shows the absorption spectra of TMB increase with the concentration of H<sub>2</sub>O<sub>2</sub> increasing, and the absorbance at 652 nm is linearly dependent on the concentration of H<sub>2</sub>O<sub>2</sub> from 0.0005 to 25 mM. Interestingly, two linear detection ranges are obtained. It is found that  $A_{652nm}$  shows a good linear relationship to H<sub>2</sub>O<sub>2</sub> concentration in a range of 0.0005–1 mM with regression coefficient ( $R^2$ ) of 0.9989 (Fig. 5c), while in the range of 1–25 mM, as shown in Fig. 5d, the  $A_{652nm}$  is proportional to the logarithmic concentration of H<sub>2</sub>O<sub>2</sub> ( $R^2 = 0.9944$ ). The limit of detection is calculated to be 0.3 μM ( $S/N = 3$ ). These results suggest that this colorimetric assay could be applied to measure the amount of H<sub>2</sub>O<sub>2</sub> in a broad range, which is superior to others reported in the literature, as listed in Table S2.

The specificity was examined by using present assay to catalyze glucose, urea, uric acid, ascorbic

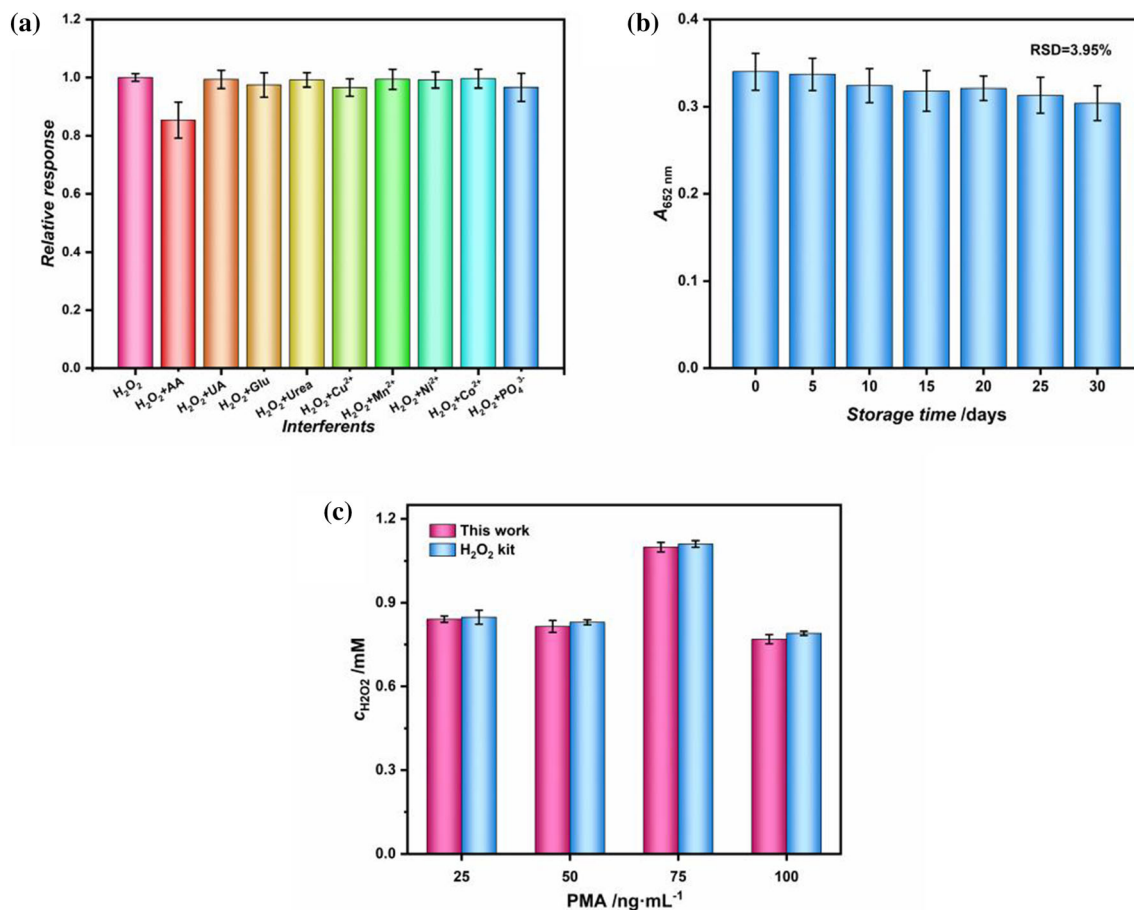


**Figure 6** **a** Normalized absorbance at 652 nm detected by Co-doped MoS<sub>2</sub> in the presence of 1 mM H<sub>2</sub>O<sub>2</sub> and other interferent species. **b** Response obtained from Co-doped MoS<sub>2</sub> measuring 1 mM H<sub>2</sub>O<sub>2</sub> after storage of different periods. **c** Comparative

analysis of the level of H<sub>2</sub>O<sub>2</sub> in SiHa cells induced by different concentrations of PMA between our proposed method and an H<sub>2</sub>O<sub>2</sub> kit. Error bars represent the standard deviations from three parallel measurements

acid, Cu<sup>2+</sup>, Mn<sup>2+</sup>, Ni<sup>2+</sup>, PO<sub>4</sub><sup>3-</sup>, respectively. Compared with H<sub>2</sub>O<sub>2</sub>, negligible interference is discovered for interferent species although their concentrations are 10 times higher than that of H<sub>2</sub>O<sub>2</sub> (Fig. 6a). In the long-term stability test, Co-doped MoS<sub>2</sub> suspension was sealed with Parafilm and stored at room temperature. Before use, the suspension was ultrasonicated for 10 min. There was no obvious decrement in A<sub>652nm</sub> for 1 mM H<sub>2</sub>O<sub>2</sub>, and 89.3% of the initial signal was retained after 30 days storage (Fig. 6b). Such observations imply that our catalytic system possesses feasibility for H<sub>2</sub>O<sub>2</sub> detection. The repeatability was investigated by detection 1 mM H<sub>2</sub>O<sub>2</sub> under optimal conditions for ten individual measurements, which yielded RSD of 2.67% (Fig. S7A). For reproducibility, five independent suspensions containing Co-doped MoS<sub>2</sub> nanosheets were synthesized under same conditions, and the

analysis of the level of H<sub>2</sub>O<sub>2</sub> in SiHa cells induced by different concentrations of PMA between our proposed method and an H<sub>2</sub>O<sub>2</sub> kit. Error bars represent the standard deviations from three parallel measurements

RSD generated from the A<sub>652nm</sub> for 1 mM H<sub>2</sub>O<sub>2</sub> was evaluated to be 4.18% (Fig. S7B). These results verify that the Co-doped MoS<sub>2</sub> nanosheets have decent repeatability and reproducibility.

### Determination of H<sub>2</sub>O<sub>2</sub> in SiHa cells

H<sub>2</sub>O<sub>2</sub> is a biomarker of cancer, which is highly expressed in cancer cells. Therefore, it is necessary to quantitatively determine H<sub>2</sub>O<sub>2</sub> and monitor the release of H<sub>2</sub>O<sub>2</sub> in cells. In our study, in situ detection of H<sub>2</sub>O<sub>2</sub> released from SiHa cells was performed using PMA as a stimulant. As shown in Fig. 6c, 75 ng/mL PMA has the strongest induction of H<sub>2</sub>O<sub>2</sub>. In comparison with the commercial H<sub>2</sub>O<sub>2</sub> kit, the detection results show no significance between the two assays with a confidence interval of 95%

( $p > 0.05$ ). These results indicate that Co-doped MoS<sub>2</sub> is feasible and reliable to detect H<sub>2</sub>O<sub>2</sub> in SiHa cells.

## Conclusions

To sum up, we have successfully synthesized a serial transition metal-doped MoS<sub>2</sub> by a facile in situ hydrothermal method and their enzyme-like activities were investigated against TMB as chromogenic substrate in the presence of H<sub>2</sub>O<sub>2</sub>. When the doping element was cobalt (Co), the highest peroxidase-like activity was obtained, which was much better than pure MoS<sub>2</sub> and other doped MoS<sub>2</sub>. Furthermore, DFT and steady-state kinetic analysis revealed the main reason for the highest peroxidase-like activity of Co-MoS<sub>2</sub>, which is due to its superior performance in electron density, active sites, adsorption and desorption capacity, affinity, and reaction rate. •O<sub>2</sub><sup>-</sup> was also confirmed to play a major role in peroxidase-mimicking reactions. Meanwhile, Co-doped MoS<sub>2</sub> exhibited long-term stability and excellent endurance and robustness under extreme environments. Two linear ranges of 0.0005–1 mM and 1–25 mM were observed for H<sub>2</sub>O<sub>2</sub> by this colorimetric assay. The detection limit is as low as 0.3 μM. Besides, in situ measurement of H<sub>2</sub>O<sub>2</sub> generated from SiHa cells was fulfilled, fully confirming the great practicability of the proposed method in biosensing fields. Our approach can also be potentially extended to design a series of other elements (such as Pt, Pd, B, N, and C)-doped MoS<sub>2</sub> as nanozymes. This work provides an alternative strategy for designing highly sensitive colorimetric sensors for biological and clinical applications. However, the poor selectivity limits the practical application of nanozyme in complicated environments. Thus, further studies such as cascading with natural enzyme and surface functionalization are progressed to circumvent the above issue.

## Funding

This work was supported by a free exploration project from the Natural Science Foundation of Shenzhen (JCYJ20170811152540640), the National Natural Science Foundation of China (81973280), and Guangdong Province Covid-19 Pandemic Control Research Fund (2020KZDZX1223).

## Declarations

**Conflict of interest** The authors declare that they have no competing interests.

**Supplementary Information:** The online version contains supplementary material available at <http://doi.org/10.1007/s10853-022-07201-z>.

## References

- [1] Aswathi R, Sandhya KY (2018) Ultrasensitive and selective electrochemical sensing of Hg(II) ions in normal and sea water using solvent exfoliated MoS<sub>2</sub>: affinity matters. *J Mater Chem A* 6:14602–14613. <https://doi.org/10.1039/c8ta00476e>
- [2] Cai SF, Han QS, Qi C, Lian Z, Jia XH, Yang R, Wang C (2016) Pt<sub>74</sub>Ag<sub>26</sub> nanoparticle-decorated ultrathin MoS<sub>2</sub> nanosheets as novel peroxidase mimics for highly selective colorimetric detection of H<sub>2</sub>O<sub>2</sub> and glucose. *Nanoscale* 8:3685–3693. <https://doi.org/10.1039/c5nr08038j>
- [3] Cai S, Fu Z, Xiao W, Xiong Y, Wang C, Yang R (2020) Zero-dimensional/Two-dimensional Au<sub>x</sub>Pd<sub>100-x</sub> nanocomposites with enhanced nanozyme catalysis for sensitive glucose detection. *ACS Appl Mater Interfaces* 12:11616–11624. <https://doi.org/10.1021/acsami.9b21621>
- [4] Cheng A, Zhang HY, Zhong WH, Li ZP, Cheng DJ, Lin YX, Tang YD, Shao HY, Li ZH (2020) Few-layer MoS<sub>2</sub> embedded in N-doped carbon fibers with interconnected macropores for ultrafast sodium storage. *Carbon* 168:691–700. <https://doi.org/10.1016/j.carbon.2020.07.008>
- [5] Ding Y, Ren G, Wang G, Lu M, Liu J, Li K, Lin Y (2020) V<sub>2</sub>O<sub>5</sub> nanobelts mimic tandem enzymes to achieve nonenzymatic online monitoring of glucose in living rat brain. *Anal Chem* 92:4583–4591. <https://doi.org/10.1021/acs.analchem.9b05872>
- [6] Dou B, Yang J, Yuan R, Xiang Y (2018) Trimetallic hybrid nanoflower-decorated MoS<sub>2</sub> Nanosheet sensor for direct in situ monitoring of H<sub>2</sub>O<sub>2</sub> secreted from live cancer cells. *Anal Chem* 90:5945–5950. <https://doi.org/10.1021/acs.analchem.8b00894>
- [7] Fan K, Xi J, Fan L, Wang P, Zhu C, Tang Y, Xu X, Liang M, Jiang B, Yan X, Gao L (2018) In vivo guiding nitrogen-doped carbon nanozyme for tumor catalytic therapy. *Nat Commun* 9:1440. <https://doi.org/10.1038/s41467-018-03903-8>
- [8] Gao L, Zhuang J, Nie L, Zhang J, Zhang Y, Gu N, Wang T, Feng J, Yang D, Perrett S, Yan X (2007) Intrinsic

- peroxidase-like activity of ferromagnetic nanoparticles. *Nat Nanotechnol* 2:577–583. <https://doi.org/10.1038/nnano.2007.260>
- [9] Guo SH, Li XH, Ren XG, Yang L, Zhu JM, Wei BQ (2018) Optical and electrical enhancement of hydrogen evolution by MoS<sub>2</sub>@MoO<sub>3</sub> core-shell nanowires with designed tunable plasmon resonance. *Adv Funct Mater* 28:1802567. <https://doi.org/10.1002/adfm.201802567>
- [10] Huang N, Peng R, Ding Y, Yan S, Li G, Sun P, Sun X, Liu X, Yu H (2019) Facile chemical-vapour-deposition synthesis of vertically aligned Co-doped MoS<sub>2</sub> nanosheets as an efficient catalyst for triiodide reduction and hydrogen evolution reaction. *J Catal* 373:250–259. <https://doi.org/10.1016/j.jcat.2019.04.007>
- [11] Jiao L, Xu W, Yan H, Wu Y, Liu C, Du D, Lin Y, Zhu C (2019) Fe-N-C single-atom nanozymes for the intracellular hydrogen peroxide detection. *Anal Chem* 91:11994–11999. <https://doi.org/10.1021/acs.analchem.9b02901>
- [12] Lazanas AC, Prodromidis MI (2021) Two-dimensional inorganic nanosheets: production and utility in the development of novel electrochemical (bio)sensors and gas-sensing applications. *Microchim Acta* 188:6. <https://doi.org/10.1007/s00604-020-04674-0>
- [13] Lei Y, Butler D, Lucking MC, Zhang F, Xia TN, Fujisawa K, Granzier-Nakajima T, Cruz-Silva R, Endo M, Terrones H, Terrones M, Ebrahimi A (2020) Single-atom doping of MoS<sub>2</sub> with manganese enables ultrasensitive detection of dopamine: experimental and computational approach. *Sci Adv* 6:32. <https://doi.org/10.1126/sciadv.abc4250>
- [14] Li HH, Zhang P, Liang CL, Yang J, Zhou M, Lu XH, Hope GA (2012) Facile electrochemical synthesis of tellurium nanorods and their photoconductive properties. *Cryst Res Technol* 47:1069–1074. <https://doi.org/10.1002/crat.201200273>
- [15] Li Z, Xin Y, Wu W, Fu B, Zhang Z (2016) Topotactic conversion of copper(I) phosphide nanowires for sensitive electrochemical detection of H<sub>2</sub>O<sub>2</sub> release from living cells. *Anal Chem* 88:7724–7729. <https://doi.org/10.1021/acs.analchem.6b01637>
- [16] Li Y, Kang Z, Kong L, Shi H, Zhang Y, Cui M, Yang DP (2019) MXene-Ti<sub>3</sub>C<sub>2</sub>/CuS nanocomposites: enhanced peroxidase-like activity and sensitive colorimetric cholesterol detection. *Mater Sci Eng C* 104:110000. <https://doi.org/10.1016/j.msec.2019.110000>
- [17] Li Y, Luo G, Qing Z, Li X, Zou Z, Yang R (2019) Colorimetric aminotriazole assay based on catalase deactivation-dependent longitudinal etching of gold nanorods. *Microchim Acta* 186:565. <https://doi.org/10.1007/s00604-019-3677-1>
- [18] Li DL, Li WL, Zhang JP (2019) Al doped MoS<sub>2</sub> monolayer: A promising low-cost single atom catalyst for CO oxidation. *Appl Surf Sci* 484:1297–1303. <https://doi.org/10.1016/j.apsusc.2019.02.016>
- [19] Liu X, Li L, Wei Y, Zheng Y, Xiao Q, Feng B (2015) Facile synthesis of boron- and nitride-doped MoS<sub>2</sub> nanosheets as fluorescent probes for the ultrafast, sensitive, and label-free detection of Hg<sup>2+</sup>. *Analyst* 140:4654–4661. <https://doi.org/10.1039/c5an00641d>
- [20] Liu Q, He Z, Wang H, Feng X, Han P (2020) Magnetically controlled colorimetric aptasensor for chlorpyrifos based on copper-based metal-organic framework nanoparticles with peroxidase mimetic property. *Microchim Acta* 187:524. <https://doi.org/10.1007/s00604-020-04499-x>
- [21] Ma C, Ma Y, Sun Y, Lu Y, Tian E, Lan J, Li J, Ye W, Zhang H (2019) Colorimetric determination of Hg<sup>2+</sup> in environmental water based on the Hg<sup>2+</sup>-stimulated peroxidase mimetic activity of MoS<sub>2</sub>-Au composites. *J Coll Interface Sci* 537:554–561. <https://doi.org/10.1016/j.jcis.2018.11.069>
- [22] Miao Z, Jiang S, Ding M, Sun S, Ma Y, Younis MR, He G, Wang J, Lin J, Cao Z, Huang P, Zha Z (2020) Ultrasmall rhodium nanozyme with RONS scavenging and photothermal activities for anti-inflammation and antitumor theranostics of colon diseases. *Nano Lett* 20:3079–3089. <https://doi.org/10.1021/acs.nanolett.9b05035>
- [23] Panferov VG, Byzova NA, Zherdev AV, Dzantiev BB (2021) Peroxidase-mimicking nanozyme with surface-dispersed Pt atoms for the colorimetric lateral flow immunoassay of C-reactive protein. *Microchim Acta* 188:309. <https://doi.org/10.1007/s00604-021-04968-x>
- [24] Raza A, Ikram M, Aqeel M, Imran M, UI-Hamid A, Riaz KN, Ali S (2020) Enhanced industrial dye degradation using Co doped in chemically exfoliated MoS<sub>2</sub> nanosheets. *Appl Nanosci* 10:1535–1544. <https://doi.org/10.1007/s13204-019-01239-3>
- [25] Ruan X, Liu D, Niu X, Wang Y, Simpson CD, Cheng N, Du D, Lin Y (2019) 2D Graphene Oxide/Fe-MOF nanozyme nest with superior peroxidase-like activity and its application for detection of woodsmoke exposure biomarker. *Anal Chem* 91:13847–13854. <https://doi.org/10.1021/acs.analchem.9b03321>
- [26] Shi Y, Zhou Y, Yang DR, Xu WX, Wang C, Wang FB, Xu JJ, Xia XH, Chen HY (2017) Energy level engineering of MoS<sub>2</sub> by transition-metal doping for accelerating hydrogen evolution reaction. *J Am Chem Soc* 139:15479–15485. <https://doi.org/10.1021/jacs.7b08881>
- [27] Taufik A, Asakura Y, Hasegawa T, Kato H, Kakihana M, Hirata S, Inada M, Yin S (2020) Surface engineering of 1T/2H-MoS<sub>2</sub> nanoparticles by O<sub>2</sub> plasma irradiation as a potential humidity sensor for breathing and skin monitoring applications. *ACS Appl Nano Mater* 3:7835–7846. <https://doi.org/10.1021/acsnm.0c01352>



- [28] Wang Q, Chen J, Zhang H, Wu W, Zhang Z, Dong S (2018) Porous  $\text{Co}_3\text{O}_4$  nanoplates with pH-switchable peroxidase- and catalase-like activity. *Nanoscale* 10:19140–19146. <https://doi.org/10.1039/c8nr06162a>
- [29] Wang Y, Qi K, Yu S, Jia G, Cheng Z, Zheng L, Wu Q, Bao Q, Wang Q, Zhao J, Cui X, Zheng W (2019) Revealing the intrinsic peroxidase-like catalytic mechanism of heterogeneous single-atom Co– $\text{MoS}_2$ . *Nano-Micro Lett* 11:102. <https://doi.org/10.1007/s40820-019-0324-7>
- [30] Wang Z, Ju P, Zhang Y, Jiang F, Ding H, Sun C (2020)  $\text{CoMoO}_4$  nanobelts as efficient peroxidase mimics for the colorimetric determination of  $\text{H}_2\text{O}_2$ . *Microchim Acta* 187:424. <https://doi.org/10.1007/s00604-020-04376-7>
- [31] Wang KC, Zhan ZX, Gao ML, Lei T, Yin P (2020) Nitrogen-doped carbon fiber/carbon paper supported Co– $\text{MoS}_2$  as an efficient catalyst for hydrogen evolution. *Mater Lett* 281:128579. <https://doi.org/10.1016/j.matlet.2020.128579>
- [32] Yang R, Fu S, Li R, Zhang L, Xu Z, Cao Y, Cui H, Kang Y, Xue P (2021) Facile engineering of silk fibroin capped AuPt bimetallic nanozyme responsive to tumor microenvironmental factors for enhanced nanocatalytic therapy. *Theranostics* 11:107–116. <https://doi.org/10.7150/thno.50486>
- [33] Zhang X, Selkirk A, Zhang S, Huang J, Li Y, Xie Y, Dong N, Cui Y, Zhang L, Blau WJ, Wang J (2017)  $\text{MoS}_2$ /carbon nanotube core-shell nanocomposites for enhanced nonlinear optical performance. *Chem Eur J* 23:3321–3327. <https://doi.org/10.1002/chem.201604395>
- [34] Zhao Z, Huang Y, Liu W, Ye F, Zhao S (2020) Immobilized glucose oxidase on boronic acid-functionalized hierarchically porous MOF as an integrated nanozyme for one-step glucose detection. *ACS Sustain Chem Eng* 8:4481–4488. <https://doi.org/10.1021/acssuschemeng.9b07631>
- [35] Zhi L, Zuo W, Chen F, Wang B (2016) 3D  $\text{MoS}_2$  composition aerogels as chemosensors and adsorbents for colorimetric detection and high-capacity adsorption of  $\text{Hg}^{2+}$ . *ACS Sustain Chem Eng* 4:3398–3408. <https://doi.org/10.1021/acssuschemeng.6b00409>
- [36] Zhu Y, Wu J, Han L, Wang X, Li W, Guo H, Wei H (2020) Nanozyme sensor arrays based on heteroatom-doped graphene for detecting pesticides. *Anal Chem* 92:7444–7452. <https://doi.org/10.1021/acs.analchem.9b05110>
- [37] Zhu J, Luo G, Xi X, Wang Y, Selvaraj JN, Wen W, Zhang X, Wang S (2021)  $\text{Cu}^{2+}$ -modified hollow carbon nanospheres: an unusual nanozyme with enhanced peroxidase-like activity. *Microchim Acta* 188:8. <https://doi.org/10.1007/s00604-020-04690-0>

**Publisher's Note** Springer Nature remains neutral with regard to jurisdictional claims in published maps and institutional affiliations.